YWHAB is regulated by IRX5 and inhibits the migration and invasion of breast cancer cells

XUEXIA GENG, JUN YUAN, WENJIE XU, DENG ZOU, YUXUAN SUN and JUN LI

School of Life Science, Huaibei Normal University, Huaibei, Anhui 235000, P.R. China

Abstract. Highly metastatic and heterogeneous breast cancer affects the health of women worldwide. Abnormal expression of tyrosine 3-monooxygenase/tryptophan 5-monooxygenase activation protein β (YWHAB), also known as 14-3-3β, is associated with the tumorigenesis and progression of bladder cancer, lung cancer and hepatocellular carcinoma; however, to the best of our knowledge, the role of *YWHAB* in breast cancer remains unknown. In the present study, a dual luciferase assay demonstrated that the transcription factor iroquois homeobox 5 may regulate *YWHAB* expression by affecting the promoter sequence upstream of its transcription start site. Subsequently, it was demonstrated that overexpression of *YWHAB* did not affect proliferation, but did reduce the migration and invasion of MDA-MB-231 cells. Furthermore, knockdown of *YWHAB* promoted the migration and invasion of MCF7 cells. Transcriptomics analysis demonstrated that when *YWHAB* was overexpressed, 61 genes were differentially expressed, of which 43 genes were upregulated and 18 genes were downregulated. These differentially expressed genes (DEGs) were enriched in cancer-related pathways, such as 'TNF signaling pathway' [Kyoto Encyclopedia of Genes and Genomes (KEGG): map04688]. The pathway with the largest number of DEGs was 'Rheumatoid arthritis' (KEGG: map05323). Notably, *YWHAB* downregulated vimentin, which is a mesenchymal marker, thus suggesting that it may weaken the mesenchymal properties of cells. These findings indicate that *YWHAB* may be a potential therapeutic target in breast cancer and further work should be performed to assess its actions as a potential tumor suppressor.

Introduction

Breast cancer is the most prevalent malignancy and the most commonly diagnosed disease in women (11.7% of total cancer cases), and its incidence has increased rapidly in recent years (1,2). Cancer recurrence and metastases are the primary factors accounting for high mortality in patients with breast cancer (3). Metastasis occurs when tumor cells acquire the ability to spread from the primary tumor site and to invade surrounding stromal tissue (4). Approximately 90% of cancer-related mortalities are due to metastasis, and in the context of tumorigenesis, epithelial-mesenchymal transition (EMT) is a critical step in the early metastatic cascade (5,6). To address these challenges, targeted therapy and anticancer drugs are still the two most promising avenues for breast cancer treatment. Alongside the well-known *BRCA1* and *BRCA2* genes, other genes have been reported to be related to breast cancer, including *FOXQ1*, *FSIP1* and *LTBP1* (7-9). Therefore, exploring the influence of genes on the ability of breast cancer to metastasize is a common research topic.

Our previous study (Geng *et al*, unpublished data) demonstrated that iroquois homeobox 5 (IRX5) could inhibit the migration and invasion of breast cancer cells and the overexpression of IRX5 may lead to high expression of tyrosine 3-monooxygenase/tryptophan 5-monooxygenase activation protein β (YWHAB). This suggests that *IRX5* may regulate the expression of *YWHAB*. Promoters regulate gene transcription at the most basic level, and thus, affect gene expression (10). Therefore, *IRX5* may regulate the expression of *YWHAB* by affecting the promoter of *YWHAB*. YWHAB is a member of the 14-3-3 protein family, which is crucial for cell proliferation, and has seven isoforms in mammals, including β, γ, ε, η, σ, τ/θ and ζ, which can assemble into homodimers or heterodimers to regulate the activities of their binding partners (11). These proteins not only serve as signaling integration points for cell cycle control and apoptosis, but also serve an essential role in health, disease and drug development. Furthermore, these proteins regulate the proliferation and migration of cancer and are upregulated in numerous types of cancer (12-14). The *YWHAB* gene encodes the 14-3-3β protein, which is involved in cell cycle control and apoptosis, and functions differently in numerous cancer types. The 14-3-3β protein has been reported to be involved in the induction of bladder cancer cell phase arrest (15), in the tumorigenesis and metastasis of lung cancer (16) and in the proliferation and apoptosis of glioma

Correspondence to: Dr Jun Li, School of Life Science, Huaibei Normal University, 100 Dongshan Road, Huaibei, Anhui 235000, P.R. China
E-mail: healthlicn@chnu.edu.cn

cells (17,18). Furthermore, *YWHAB* is a biomarker in hepatocellular carcinoma (19). Although *YWHAB* serves different roles in different cancer types, its specific mechanism requires further investigation. Notably, to the best of our knowledge, there are no studies assessing the role of *YWHAB* in breast cancer.

The present study explored the regulatory effect of *IRX5* on *YWHAB* using a dual-luciferase reporter gene assay. *YWHAB* expression was altered by lentiviral transduction *in vitro* and the biological function of *YWHAB* was assessed.

Materials and methods

Bioinformatics. The University of Alabama at Birmingham Cancer data analysis portal (UALCAN; https://ualcan.path. uab.edu/analysis.html) was used to analyze the expression levels of *IRX5* and *YWHAB* in different subtypes of breast cancer cells in The Cancer Genome Atlas (TCGA) database. The dataset used was TCGA dataset: Breast invasive carcinoma in UALCAN. Gene Expression Profiling Interactive Analysis (GEPIA; http://gepia.cancer-pku.cn/index.html) was used to analyze the correlation between YWHAB and IRX5 expression in breast cancer. The dataset used was breast invasive carcinoma (BRCA) tumor (BRCA: breast cancer) in GEPIA.

Cell culture. MDA-MB-231, MCF7 and 293FT cell lines were purchased from Procell Life Science & Technology Co. Ltd. The MDA-MB-231 cells were cultured in DMEM/F12 (Gibco; Thermo Fisher Scientific, Inc.) containing 10% FBS (MilliporeSigma), 100 U/ml penicillin and 100 μg/ml streptomycin. The MCF7 and 293FT cells were cultured in DMEM (Gibco; Thermo Fisher Scientific, Inc.) supplemented with 10% FBS, 100 U/ml penicillin and 100 μg/ml streptomycin (Gibco; Thermo Fisher Scientific, Inc.). All cells were cultured in a saturated humidity incubator containing 5% CO_2 at 37˚C.

Dual luciferase assay. The promoter sequence upstream of the human *YWHAB* transcription start site (NC_000020.11: 44883702-44885654) was obtained by PCR amplification. 293FT cell genomic DNA as the PCR template was extracted using the Genomic DNA Mini-Preps Kit (Beijing Baiolaibo Technology Co., Ltd.). Prime STAR GXL DNA Polymerase, dNTP Mixture and 5X PrimeSTAR GXL Buffer were purchased from Takara Biotechnology Co., Ltd. The primers used are shown in Table I. The PCR reaction procedure was as follows: 98˚C for 2 min, followed by 30 cycles of 98˚C for 10 sec, 50˚C for 15 sec and 68˚C for 2 min; and final extension at 68˚C for 10 min. PCR products were detected using a 1% agarose gel containing ethidium bromide and bands were observed using a gel imaging system (ProteinSimple). Finally, the correctness of the sequence was verified by Sanger sequencing (Sangon Biotech Co., Ltd.). The YWHAB-promoter-PGL3 vector was obtained by ligating the promoter sequence into the pGL3-basic vector (Promega Corporation). The open reading frames of the *IRX5* (NM_005853.6) gene were cloned into a pcDNA3.1(+) vector (Invitrogen; Thermo Fisher Scientific, Inc.). For the luciferase assay, 5x10⁴ 293FT cells were plated and cultured in 24-well plates overnight at 37˚C until they reached 80% confluence, after which, they were co-transfected with YWHAB-promoter-PGL3 vector, pcDNA3.1-IRX5 vector and PGMR-TK *Renilla* luciferase reporter plasmid (Genomeditech) using Lipofectamine 2000 (Thermo Fisher Scientific, Inc.). Firefly and *Renilla* luciferase activity were measured after transfection for 24 h using a Dual Luciferase Reporter Gene Assay Kit (Beyotime Institute of Biotechnology).

Lentivirus transduction and stable cell line construction. The coding sequences (CDSs) of the *YWHAB* gene (GenBank NM_139323.4) were obtained by reverse transcription-PCR (RT-PCR) and were checked by Sanger sequencing (Sangon Biotech Co., Ltd.). RNAiso Plus reagent (Takara Biotechnology Co., Ltd.) was used to extracted RNA from 293FT cells, and the PrimeScriptTMRT reagent Kit with gDNA Eraser (Takara Biotechnology Co., Ltd.) was used to reverse transcribe RNA into cDNA. The primers used are shown in Table I. The PCR reaction procedure used was as follows: 98˚C for 2 min; 98˚C for 30 sec, 50˚C for 30 sec and 68˚C for 1 min for 30 cycles; 68˚C for 1 min. The verified CDSs were ligated into the lentiviral vector PEB-3XFlag-GP (Guangzhou Huijun Biotechnology Co., Ltd.) and were packaged using the GM easy™ lentiviral Packaging Kit (Genomeditech; third-generation lentiviral packaging system). The lentiviral transduction plasmid:packaging plasmid:envelope plasmid ratio was 2:1:1. Briefly, 10 μg of the aforementioned recombinant plasmid and 10 μg of the GM easy™ Lentiviral Mix plasmid (Genomeditech) were co-transfected into 293FT cells (10-cm Petri dish; 80% confluence) using 60 μl HG Transgene™ Reagent (Genomeditech). The cells were cultured at 37˚C with 5% CO_2 for 18 h and then the culture medium was replaced. After culturing for 48 h, the supernatant was collected and contained the lentiviral particles. The lentiviral particles (MOI, 20) were added to MDA-MB-231 cells and the culture medium was replaced 12 h later. Empty PEB-3XFlag-GP was packaged and transduced simultaneously as a control. After 48 h, puromycin (2 μg/ml) was used for selection for 2 weeks and 0.5 μg/ml puromycin was used for maintenance. The time interval between transfection and subsequent experimentation was 14 days. Western blotting and RT-quantitative PCR (RT-qPCR) were used to detect the *YWHAB* transduction efficiency. MDA-MB-231 cells were transduced with the empty lentiviral vector or *YWHAB*-linked lentiviral vector and were named MDA-MB-231-VC and MDA-MB-231-YWHAB, respectively. The lentiviral vector used to knock down *YWHAB* was purchased from Guangzhou IGE Biotechnology Co., Ltd. The short hairpin RNA (sh) sequence targeting *YWHAB* and the scrambled negative control are shown in Table I. Lentiviral packaging and transduction were performed in the aforementioned manner. The MCF7 cells with knockdown of *YWHAB* were referred to as MCF7-shYWHAB cells, and the control cells were referred to as MCF7-CT cells.

RNA extraction and RT-qPCR. Total RNA was extracted from MDA-MB-231, MCF7 and 293FT cells using RNAiso Plus reagent (Takara Biotech Co., Ltd.) and was reverse transcribed into cDNA using the PrimeScript™ RT reagent Kit with gDNA Eraser (Takara Biotechnology Co., Ltd.) according to the manufacturer's instructions. qPCR was performed using

Table I. Primers and shRNA sequences used in the present study.

Assay	Gene	Sequence (5'-3')
PCR	YWHAB-promoter	GGGGTACCGTGGCACAGTACAGGGGTCA
		CCCAAGGCTTCCTCGCCTTCACCGCTAGCC
RT-PCR	YWHAB	F:GCTCTAGACACCATGACAATGGATAAAAGTGAGC
		R: CGGGATCCGTTCTCTCCCTCCCCAGCGT
RT-qPCR	GAPDH	F: ACACCCACTCCTCCACCTTT
		R: TTACTCCTTGGAGGCCATGT
	YWHAB	F: CACAGAACAGGGGCATGAAC
		R: GTCCTGCAGTTCTGCCTCT
	FAM20C	F: TGTTCAAACCCATGAAACAAACG
		R: GTAGTAGGAACACTCGCCGT
	PLEC	F: AGCACCTCATCAAGGCCCAG
		R: TTGTCCAGATGAGGCCAAGG
	MMP1	F: TACCTGGAAAAATACTACAACCTGA
		R: GGCGTGTAATTTTCAATCCTGTAG
	DDIT3	F: AACCTGAGGAGAGAGTGTTCA
		R: TAATGGGGAGTGGCTGGAAC
	HERPUD1	F: CGAGATTGGTTGGATTGGACCT
		R: TTTCAGGATCAGTGCCTTCCTGT
	MMP3	F: TGGACAAAGGATACAACAGGGAC
		R: ATCTTGAGACAGGCGGAACC
	IL24	F: ACAGGACCAGAGGGACAAGA
		R: AGGGTAAAACCCAGGCAAGG
	TNFSF15	F: GGATCTGGGACTGAGCTTTGG
		R: CCTGTCCTTTTAGAGCCTGGAAC
shRNA	shYWHAB	CCGGCCAATGCTACACAACCAGAAACTCGAGTTT
		CTGGTTGTGTAGCATTGGTTTTTGAATTC
	sh-scramble	CCGGTCCTAAGGTTAAGTCGCCCTCGCTCGAGCGA
		GGGCGACTTAACCTTAGGTTTTTGAATTC

Underlining indicates parts that are complementary or identical to the *YWHAB* sequence. F, forward; R, reverse; RT-PCR, reverse transcription-PCR; RT-qPCR, reverse transcription-quantitative PCR; shRNA/sh, short hairpin RNA.

the 2X SG Fast qPCR Master Mix Kit (Sangon Biotech Co., Ltd.) on a LightCycler96 (Roche Diagnostics) with the following thermocycling conditions: Initial denaturation at 95°C for 5 min, followed by 40 cycles of 95°C for 3 sec, 60°C for 30 sec and 97°C for 1 sec. mRNA levels were quantified using the $2^{-\Delta\Delta Cq}$ method and normalized to the internal reference gene *GAPDH* (20). The primers used in the present study are shown in Table I.

Western blotting. Proteins were extracted from cells (MDA-MB-231-VC, MDA-MB-231-YWHAB, MCF7-CT and MCF7-shYWHAB cells) using RIPA lysis buffer (Beyotime Institute of Biotechnology). Total protein was quantified using the BCA Protein Assay Kit (Beyotime Institute of Biotechnology) and the concentration was then adjusted to 4 μg/μl. The proteins (60 μg/lane) were separated by SDS-PAGE on a 10% gel and then transferred onto PVDF membranes (MilliporeSigma) for 90 min at 4°C at 150 mAh, and the membranes were blocked with 5% non-fat milk for 1 h at room temperature and incubated with the following

primary antibodies overnight at 4°C: Mouse anti-Flag (1:1,000; cat. no. D191041; Sangon Biotech Co., Ltd.), rabbit anti-vimentin (1:1,000; cat. no. 5741T; Cell Signaling Technology, Inc.), rabbit anti-YWHAB (1:1,000; cat. no. BM4752; Boster Biological Technology) and mouse anti-GAPDH (1:1,000; cat. no. D190090; Sangon Biotech Co., Ltd.). The membranes were then washed three times with TBS with 0.1% Tween-20 and incubated with the following HRP-conjugated secondary antibodies at 4°C for 2 h: HRP-conjugated Goat Anti-Mouse (1:5,000; cat. no. D110087; Sangon Biotech Co., Ltd.) and HRP-conjugated Goat Anti-Rabbit (1:5,000; cat. no. D110058; Sangon Biotech Co., Ltd.). The antibody against the Flag tag was used to examine the exogenous YWHAB protein with the Flag tag. Finally, an HRP-DAB color development kit (Tiangen Biotech Co., Ltd.) or ultrasensitive luminescence reagent (Sangon Biotech Co., Ltd.) was used for visualization. Images were captured using an image analysis system (5200; Tanon Science and Technology Co., Ltd.) and protein bands were semi-quantified using ImageJ 1.8 (National Institutes of Health).

MTT cell proliferation assay. The MTT assay was performed to examine cell proliferation. MDA-MB-231-VC and MDA-MB-231-YWHAB cells were seeded at a density of $5x10^3$ cells/well in 96-well plates and cultured for 1, 2, 3, 4 and 5 days. The cells were then incubated with MTT reagent (Beijing Solarbio Science & Technology Co., Ltd.) for 4 h. DMSO (Beijing Solarbio Science & Technology Co., Ltd.) was added to each well to dissolve formazan crystals, and the absorbance was determined at 490 nm using a microplate reader (Super Max 3100; Shanghai Shanpu Biotechnology Co., Ltd.).

Cell colony formation assay. Cell colony formation was measured using a plate colony formation assay. MDA-MB-231-VC and MDA-MB-231-YWHAB cells were seeded into 6-well plates at a density of 200 cells/well and were cultured at 37°C in 5% CO_2 for 2 weeks until visible cell colonies were formed. Cells were washed with PBS and fixed in 4% paraformaldehyde for 15 min at room temperature. Before counting, the cell colonies were gently washed with PBS and then stained with 0.1% crystal violet for 15 min at room temperature. Viable colonies containing ≥50 cells were counted manually using an inverted light microscope (DP72; Olympus Corporation).

Wound healing assay. To assess breast cancer cell migration, a wound healing assay was performed. MDA-MB-231-VC and MDA-MB-231-YWHAB cells were seeded in 6-well plates at a density of $2x10^5$ cells/well and were cultured at 37°C for 24 h. When the cells achieved stable attachment and reached 90% confluence, a parallel linear scratch was generated using a sterile 200-μl pipette tip. After rinsing with PBS, the wounded cells were cultured in serum-free DMEM (Gibco; Thermo Fisher Scientific, Inc.). Images were captured using an inverted light microscope (DP72; Olympus Corporation) after 0, 24 and 48 h of incubation at 37°C. The areas were measured using ImageJ 1.8 (National Institutes of Health). The cell wound healing rate can reflect migration, and was calculated as follows: Relative migration rate (%)=closure area/initial area x100%.

Cell migration and invasion assays. Cell invasion and migration were assessed using 24-well Transwell plates (8-μm pore size; Corning, Inc.) and a Cell Invasion Chamber (8-μm pore size; Beijing Labselect). The pre-coating with Matrigel of the Cell Invasion Chamber was completed by the manufacturer. Cells ($5x10^4$; MDA-MB-231-VC, MDA-MB-231-YWHAB, MCF7-CT and MCF7-shYWHAB cells) were collected and seeded into the upper chambers in serum-free culture medium. Medium containing 10% FBS was added to the lower chambers to attract cells migrating and invading through the membranes. After incubation at 37°C for 24 h, the cells in the upper chambers were removed by washing with PBS. The cells that had migrated and invaded through the membranes of the chambers were fixed with paraformaldehyde at room temperature for 15 min, stained with crystal violet at room temperature for 15 min and counted under an inverted light microscope (DP72; Olympus Corporation).

Kyoto Encyclopedia of Genes and Genomes (KEGG) and Gene Ontology (GO) enrichment analyses. The transcriptome analysis of MDA-MB-231-YWHAB and MDA-MB-231-VC cells was performed by Novogene Co., Ltd. Total RNA was isolated from cells using TRIzol reagent (Thermo Fisher Scientific, Inc.) according to the manufacturer's protocols. Total RNA was identified and quantified as follows: 1% agarose gel electrophoresis was used to analyze the degree of RNA degradation and DNA contamination in the sample; a spectrophotometer (NanoPhotometer; Implen GmbH) was used to measure RNA purity and concentration; RNA integrity and quantity were measured using the RNA Nano 6000 Assay Kit (Agilent Technologies, Inc.) on the Bioanalyzer 2100 system (Agilent Technologies, Inc.). The kits used to Library preparation included: ABclonal First Strand synthesis module (cat. no. RK20353L; ABclonal Biotech Co., Ltd.), ABclonal Second Strand synthesis module (cat. no. RK20346L; ABclonal Biotech Co., Ltd.) and KC-Digital Stranded mRNA Library Prep Kit for Illumina-UMI (cat. no. DR085-01/02; Seqhealth). Library quantification was performed using a Qubit2.0 fluorometer (Invitrogen; Thermo Fisher Scientific, Inc.). Libraries were sequenced with a NovaSeq 6000 S4 Reagent Kit v1.5 (300 cycles; cat. no. 20028312; Illumina, Inc.). The final library loading concentration was 5 nM. An Illumina Novaseq 6000 (Illumina, Inc.) was used to conduct paired-end sequencing with the PE150 mode according to the manufacturer's protocol. UMI-tools (v1.1.2) was used to identify the unique molecular identifier sequence on each sequence in the clean reads (21). Cleaning of reads was performed by deleting reads that contain adapter reads, plot-N reads and low-quality reads. HISAT2 v2.1.0 was used to construct a reference genome index and perform reference genome alignment on paired-end clean reads (22). StringTie (v2.2.1) was used for new gene prediction (23). FeatureCounts (v2.0.1) was used to count reads mapped to each gene (24). Differential expression analysis of the two cell groups was performed using the edgeR software package (v3.22.5) (25). The genes with a $\log_2$ fold change value >1 and P<0.05 were considered significantly differentially expressed genes (DEGs). GO (http://geneontology.org/) and KEGG (https://www.genome.jp/kegg/) enrichment analyses were performed to evaluate the biological function of *YWHAB* and to investigate the pathways in which the DEGs were involved. GO and KEGG enrichment analysis was performed using the clusterProfiler R package (3.8.1) (26).

Statistical analysis. All data were processed using the statistical software SPSS 20.0 (IBM Corp.) and GraphPad Prism 8.0 (Dotmatics). The data are presented as the mean ± SD. Differences between means were evaluated using unpaired Student's t-tests or one-way analysis of variance with Tukey's post hoc test. All experiments were repeated three times. P<0.05 was considered to indicate a statistically significant difference.

Results

IRX5 binds to the promoter of YWHAB and regulates its expression. Using TCGA, it was demonstrated that the expression levels of *IRX5* and *YWHAB* were both decreased with the increase in the metastatic ability of breast cancer cell subtypes (metastatic ability of breast cancer cell subtypes: Luminal < HER2-positive < triple-negative) (Fig. 1A). This
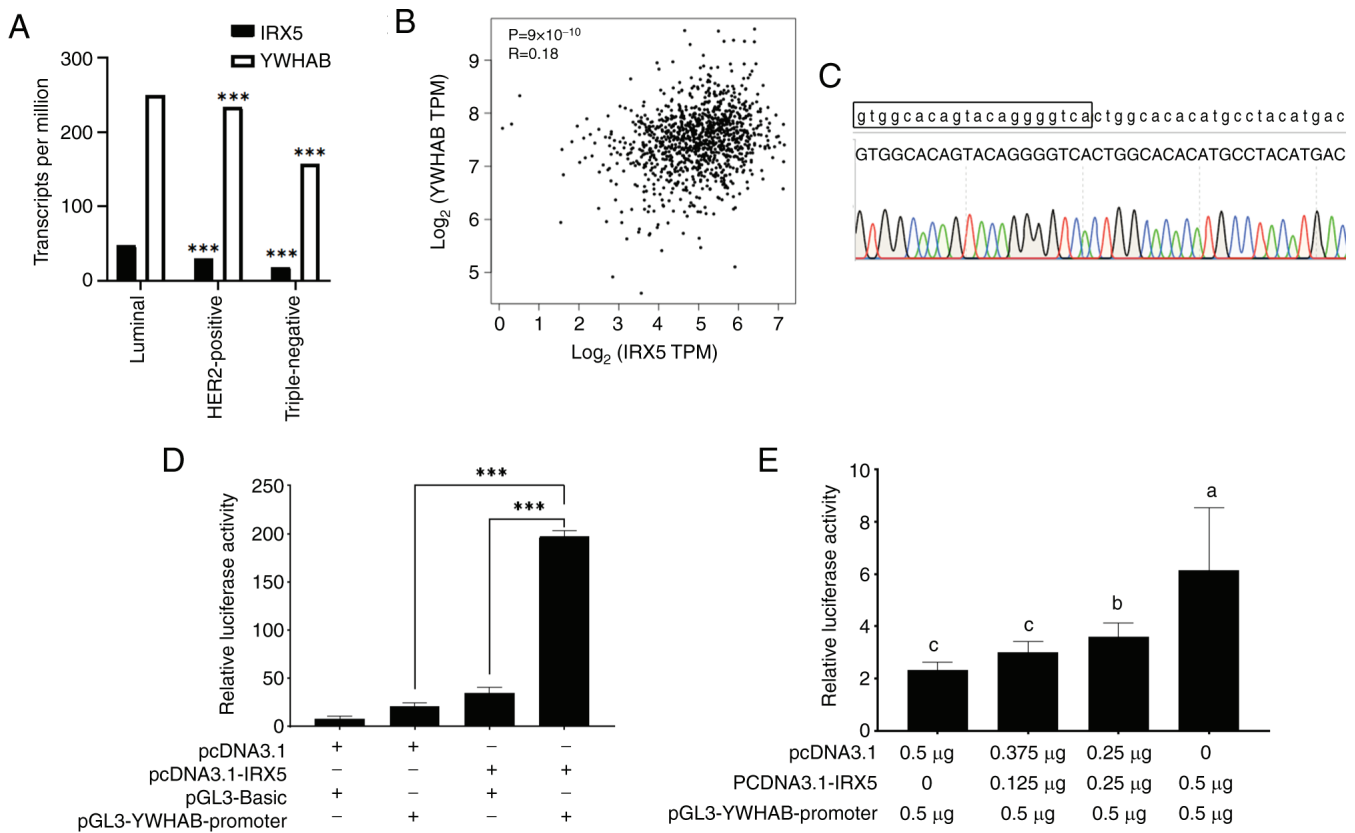
Figure 1. Dual luciferase reporter gene assay to assess the regulatory effect of IRX5 on the *YWHAB* promoter. (A) The University of Alabama at Birmingham Cancer data analysis portal was used to analyze the expression levels of *IRX5* and *YWHAB* in different subtypes of breast cancer cells. The expression level is displayed as the median value from the database. (B) Analysis of the correlation between *YWHAB* and *IRX5* expression in breast cancer using Gene Expression Profiling Interactive Analysis. (C) Representative Sanger sequencing traces of *YWHAB* promoter sequence. Lowercase letters (a t g c), *YWHAB* promoter sequence in the National Center for Biotechnology Information database. Capital letters (A T G C), Sanger sequencing results. Sequence in the box, PCR primers. (D) Dual luciferase reporter gene analysis of IRX5 protein binding to the *YWHAB* promoter. (E) Regulation of *YWHAB* promoter by pcDNA3.1-IRX5 at different concentrations. Groups with different lowercase letters are significantly different (P<0.05). ***P<0.001 vs. luminal or as indicated. IRX5, iroquois homeobox 5; TPM, transcripts per million; YWHAB, tyrosine 3-monooxygenase/tryptophan 5-monooxygenase activation protein β.

showed that the higher the metastatic ability of breast cancer subtypes, the lower the expression levels of *YWHAB* and *IRX5*. High expression of *YWHAB* may inhibit the metastatic ability of breast cancer. The very weak positive association between *YWHAB* and *IRX5* gene expression was determined by Pearson correlation analysis using GEPIA (Fig. 1B). The correctness of the *YWHAB* promoter sequences was verified using Sanger sequencing (Fig. 1C). To determine whether IRX5 interacts with the YWHAB promoter, a dual-luciferase assay was used to detect the interaction between IRX5 and the YWHAB promoter. Compared with PCDNA3.1-IRX5 or PGL3-YWHAB-promoter alone, the simultaneous addition of both significantly increased the luciferase activity (Fig. 1D). This indicated that IRX5 significantly increased luciferase activity by affecting the YWHAB promoter. 293FT cells were transfected with pcDNA3.1-IRX5 plasmid at numerous concentrations to confirm the regulatory effect on the promoter. As the concentration of pcDNA3.1-IRX5 plasmid increased, the luciferase activity also increased (Fig. 1E). These results suggested that IRX5 may regulate *YWHAB* gene expression by affecting the *YWHAB* promoter.

YWHAB does not affect breast cancer cell proliferation. To elucidate the function of *YWHAB* in breast cancer cells, *YWHAB*

was overexpressed in MDA-MB-231 cells. Sanger sequencing was performed to verify the correctness of YWHAB coding sequences (Fig. 2A). The overexpression of *YWHAB* was verified by RT-qPCR and western blotting. YWHAB mRNA expression was significantly increased in the cells transfected with the *YWHAB* overexpression plasmid compared with those transfected with the empty vector (Fig. 2B). Western blotting also demonstrated successful transduction using the Flag antibody to detect Flag-tagged YWHAB protein (Fig. 2C). The MTT assay was performed to identify the effect of *YWHAB* overexpression on cell proliferation. Cell proliferation curves demonstrated that there was no significant difference in the proliferation of cells between the YWHAB-OE and VC groups (Fig. 2D). No significant difference in colony numbers was observed between the YWHAB-OE and VC groups (Fig. 2E). These findings indicated that *YWHAB* overexpression may have no effect on breast cancer cell proliferation.

YWHAB inhibits breast cancer cell migration and invasion. The characteristics of cancer cells also include migration and invasion. The aforementioned results demonstrated that *YWHAB* had no significant effect on cell proliferation. The effect of overexpression of *YWHAB* on cell migration and invasion was assessed using wound healing and Transwell
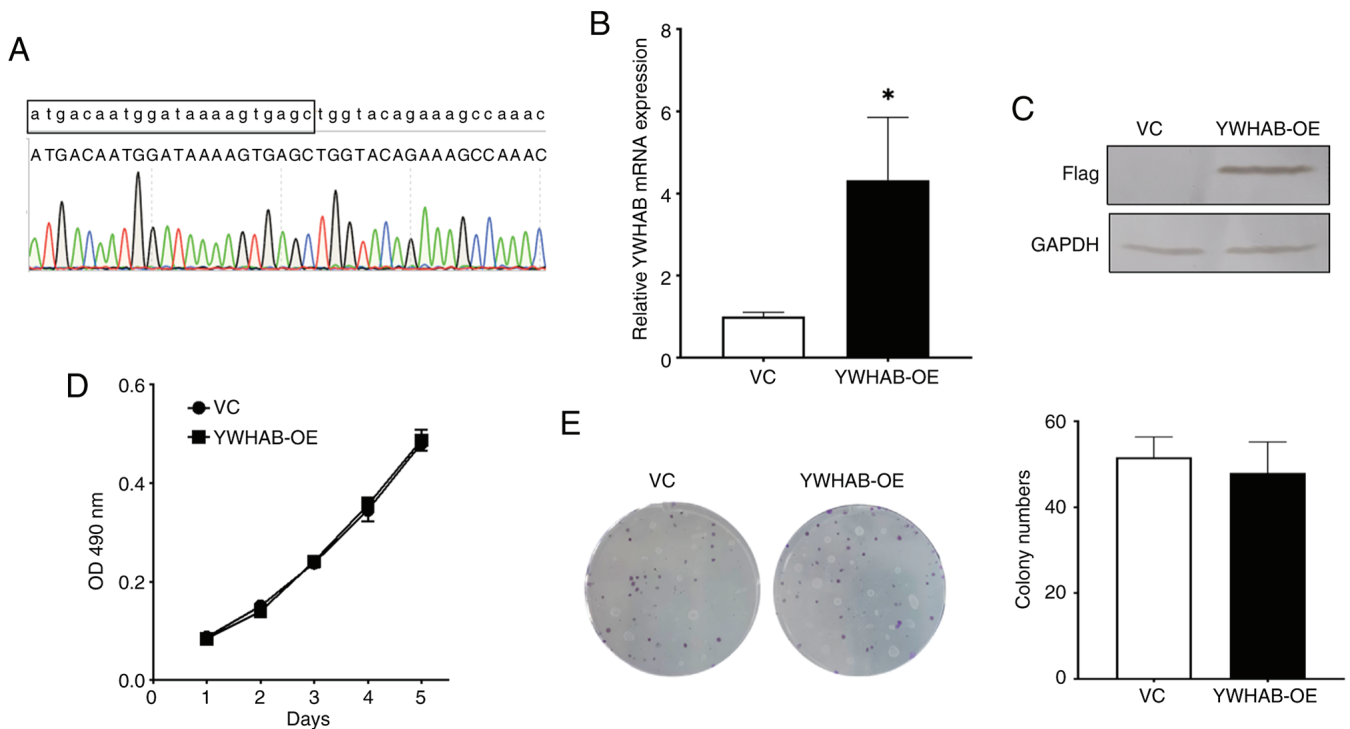
Figure 2. Effect of overexpression of *YWHAB* on the proliferation of MDA-MB-231 cells. (A) Representative Sanger sequencing traces of *YWHAB* coding sequence. Lowercase letters (a t g c), YWHAB coding sequences in the National Center for Biotechnology Information database. Capital letters (A T G C), Sanger sequencing results. Sequence in the box, RT-PCR primers. (B) Reverse transcription-quantitative PCR and (C) western blotting using the Flag antibody were performed to detect the effect of *YWHAB* overexpression on *YWHAB* expression. (D) MTT and (E) colony formation assays demonstrated the effect of *YWHAB* overexpression on cell proliferation. *$P<0.05$. OD, optical density; VC, MDA-MB-231 cells transduced with the empty lentiviral vector; YWHAB-OE, MDA-MB-231 cells overexpressing *YWHAB*; YWHAB, tyrosine 3-monooxygenase/tryptophan 5-monooxygenase activation protein β.

assays. In the wound healing assay, the relative migration rate of the YWHAB-OE group was significantly reduced at 48 h compared with that of the VC group (Fig. 3A). The Transwell assay demonstrated that YWHAB-OE significantly reduced cell migration and invasion compared with that of the VC group (Fig. 3B and C). Furthermore, *YWHAB* expression was knocked down in MCF7 breast cancer cells, which was verified by RT-qPCR and western blotting. The results demonstrated that in MCF7-shYWHAB cells, the mRNA levels of *YWHAB* were significantly reduced compared with those in the control group (Fig. 4A). Western blotting demonstrated a notable decrease in the protein levels of YWHAB in MCF7-shYWHAB cells (Fig. 4B). Furthermore, the Transwell assays demonstrated that *YWHAB* knockdown significantly increased cell migration and invasion compared with those in the control group (Fig. 4C and D). These results indicated that *YWHAB* could inhibit cell migration *in vitro*, which suggests that *YWHAB* may act as a tumor suppressor gene.

Functional enrichment analyses. To clarify the molecular pathways that are involved in YWHAB-induced suppression of cell migration and invasion, transcriptome analysis was performed in *YWHAB*-overexpressing cells and control cells. The data from this assay have been uploaded to the Gene Expression Omnibus database (GSE218458). A total of 61 genes were demonstrated to be differentially expressed, among which 43 genes were upregulated and 18 genes were downregulated when *YWHAB* was overexpressed in MDA-MB-231 cells (Fig. 5A). GO and KEGG pathway enrichment analyses were used to

assess the pathways and molecular functions in which the DEGs were involved, in order to better understand the functions of *YWHAB* overexpression. GO was used to classify gene functions where each DEG could be assigned to one or more GO terms within three domains. 'Response to stimulus' (GO:0050896), 'cellular response to stimulus' (GO:0051716) and 'localization' (GO:0051179) were enriched in the biological process domain. Within the cellular component domain, the three most enriched categories were 'extracellular region' (GO:0005576), 'extracellular region part' (GO:0044421) and 'vesicle' (GO:0031982). In terms of molecular functions, the enriched categories were 'cytokine activity' (GO:0005125), 'receptor binding' (GO:0005102) and 'extracellular matrix structural constituent' (GO:0005201) (Fig. 5B). The DEGs were mainly associated with the terms relating to the extracellular region, environmental stimuli and binding to receptors, suggesting that YWHAB may be involved in these signaling pathways affecting metastasis of cells. The DEGs were also assigned to the biological pathways described in KEGG to better understand their specific metabolic pathways in cells (Fig. 5C). The 'TNF signaling pathway' (KEGG: map04688) is related to cancer processes. The pathway with the largest number of DEGs was 'Rheumatoid arthritis' (KEGG: map05323). These results indicated that *YWHAB* and DEGs may affect the metastasis of breast cancer cells by participating in multiple signaling pathways.

By searching existing studies, three genes (*MMP1*, *MMP3* and *IL24*) related to breast cancer or EMT were selected (27-32). In the present study, both transcriptome analysis results and RT-qPCR detection indicated that *MMP1*, *MMP3* and *IL24* were
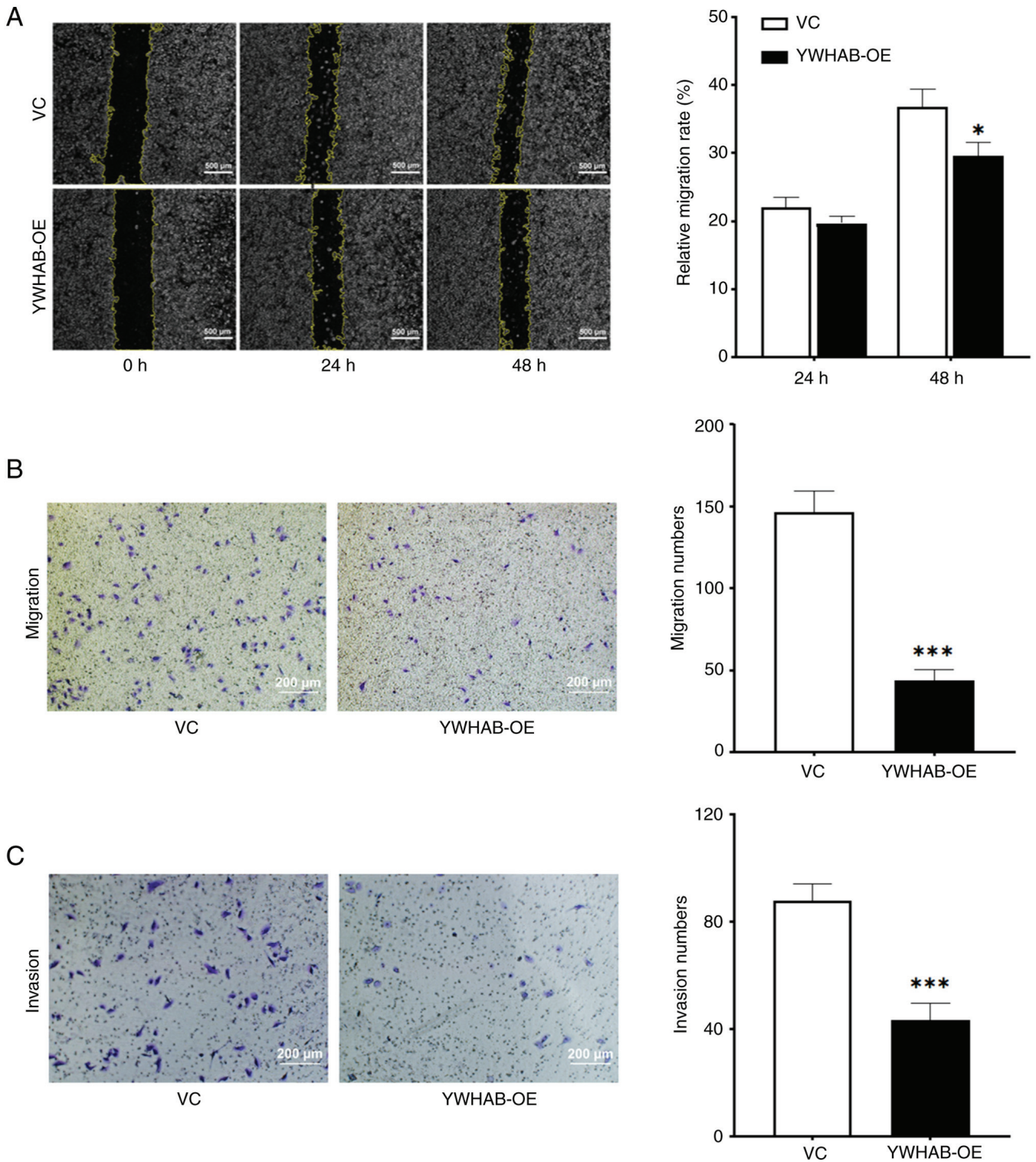
Figure 3. Effect of *YWHAB* overexpression on the migration and invasion of MDA-MB-231 breast cancer cells. (A) Wound healing assay demonstrating the effect of *YWHAB* overexpression on cell migration. Scale bar, 500 μm. Transwell assays revealed the effects of *YWHAB* overexpression on (B) migration and (C) invasion. Scale bar, 200 μm. *P<0.05 and ***P<0.001 vs. VC. VC, MDA-MB-231 cells transduced with the empty lentiviral vector; YWHAB-OE, MDA-MB-231 cells overexpressing *YWHAB*; YWHAB, tyrosine 3-monooxygenase/tryptophan 5-monooxygenase activation protein β.

downregulated (Fig. 6A). In addition, five DEGs (*FAM20C*, *PLEC*, *TNFSF15*, *DDIT3* and *HERPUD1*) were randomly selected for RT-qPCR detection to verify whether their expression changes were consistent with the transcriptome analysis results. The results showed that *FAM20C* and *PLEC* were upregulated in MDA-MB-231-YWHAB cells. *TNFSF15*, *DDIT3*

and *HERPUD1* were downregulated (Fig. 6A). The upregulation and downregulation trends of these genes detected by RT-qPCR were consistent with the trends in transcriptome analysis.

YWHAB can reduce vimentin expression. Vimentin is a mesenchymal marker that is associated with EMT (33). The
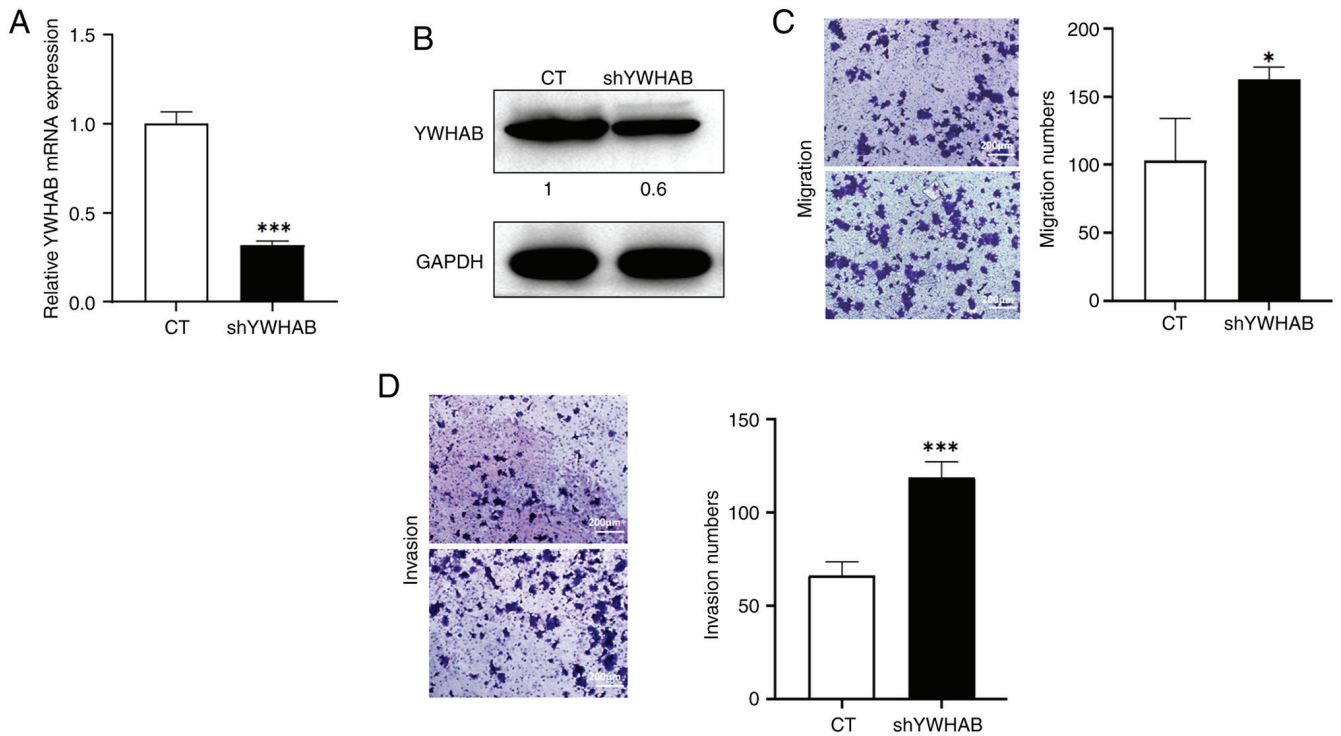
Figure 4. Effects of knockdown of *YWHAB* on the migration and invasion of MCF7 breast cancer cells. (A) Reverse transcription-quantitative PCR and (B) western blotting were used to detect the effect of *YWHAB* knockdown on MCF7 cells. Transwell assays demonstrated the effects of *YWHAB* knockdown on the (C) migration and (D) invasion of MCF7 cells. Scale bar, 200 μm. *P<0.05 and ***P<0.001. sh, short hairpin RNA; shYWHAB, MCF7 cells with *YWHAB* knockdown; CT, MCF7 cells transduced with the lentiviral vector of scrambled negative control; YWHAB, tyrosine 3-monooxygenase/tryptophan 5-monooxygenase activation protein β.

changes in vimentin expression after overexpression and knockdown of *YWHAB* were assessed. After the overexpression of *YWHAB*, the protein levels of vimentin were decreased, whereas after the knockdown of *YWHAB*, the protein levels of vimentin were increased (Fig. 6B). The aforementioned results suggest that there may be an association between *YWHAB* and vimentin.

Discussion

The incidence of breast cancer is increasing each year (1). Therefore, there is a need to evaluate the mechanism underlying breast cancer, since few molecular targets of breast cancer are known. In the present study a weak positive association between *YWHAB* and *IRX5* expression was demonstrated using GEPIA. Furthermore, the expression levels of *IRX5* and *YWHAB* were decreased with the increase in metastatic ability of breast cancer cell subtypes (luminal < HER2-positive < triple-negative). Finally, it was demonstrated that IRX5 regulates *YWHAB* gene expression via the promoter of *YWHAB*.

The IRX family of transcription factors are upstream factors identified to regulate neural gene expression in *Drosophila* (34). The IRX family contains six genes, *IRX1*, *IRX2*, *IRX3*, *IRX4*, *IRX5* and *IRX6*, in mice and humans, which encode highly conserved homologous framework structural domains (34,35), and serve pivotal roles in cell development and human cancer progression (36,37). *IRX5* functions in a variety of tumors through different signaling pathways, such as prostate cancer, hepatocellular carcinoma, tongue squamous cell carcinoma and colorectal

cancer (38-41). In our previous study (Geng *et al*, unpublished data), it was demonstrated that IRX5 could affect breast cancer cell invasion. Previous studies have reported that *YWHAB* is aberrantly expressed during cancer development. *YWHAB* is upregulated in gastric cancer, lung cancer and hepatocellular carcinoma, and is downregulated in B cell lymphoma (42-44). These findings indicated that *YWHAB* likely serves distinct roles in different malignancies and may be considered a therapeutic target for some types of cancer. *YWHAB* is also associated with proliferation, migration and invasion in hepatocellular carcinoma, gastric cancer and cervical cancer (45-47). Based on this, we hypothesized that *YWHAB* may serve a role in the development of breast cancer and may be an effective molecular therapeutic target. Therefore, MDA-MB-231 cells were selected to assess the impact of overexpression of *YWHAB*.

The results of the present study demonstrated that *YWHAB* had no effect on cell proliferation, but it inhibited the migration and invasion of cells, as determined by wound healing and Transwell assays. In general, the occurrence of apoptosis and changes in the cell cycle are accompanied by changes in cell proliferation (48). In the present study, no significant changes in cell proliferation were observed, suggesting that *YWHAB* most likely does not impact pathways involved in the cell cycle and apoptosis. Transcriptome analysis was performed to evaluate DEGs in MDA-MB-231 cells overexpressing YWHAB. The most significantly enriched pathway with the largest number of DEGs was 'Rheumatoid arthritis' (KEGG: map05323). The 'TNF signaling pathway' (KEGG: map04688) is closely related to cancer. According to the functional enrichment results, *YWHAB* may be involved in multiple signaling pathways.
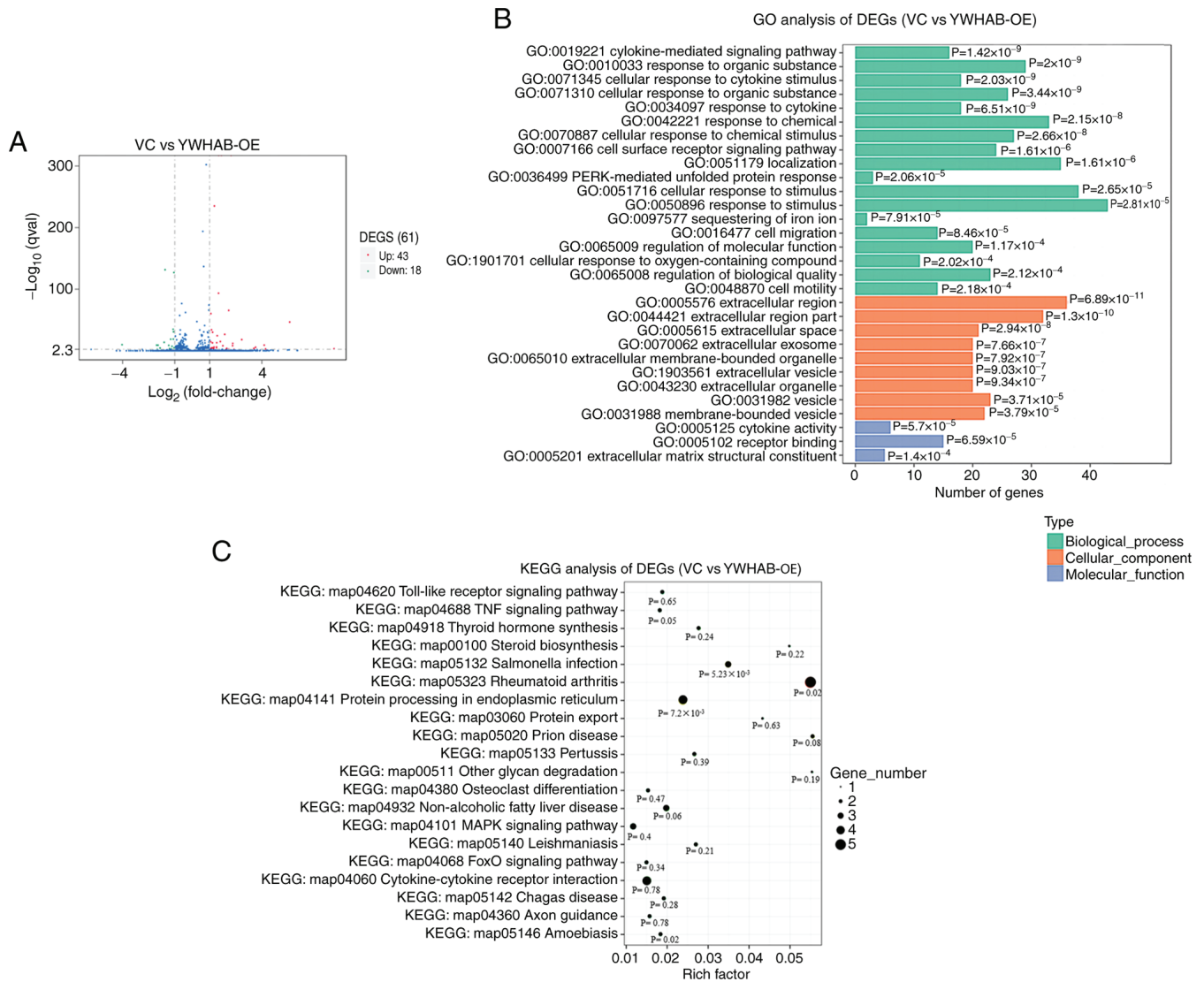
Figure 5. GO and KEGG analysis of DEGs. (A) Volcano map of DEGs. Red, upregulation; green, downregulation. (B) GO annotation map of DEGs. (C) KEGG annotation of DEGs. DEGs, differentially expressed genes; GO, Gene Ontology; KEGG, Kyoto Encyclopedia of Genes and Genomes; PERK, protein kinase RNA-like ER kinase; VC, MDA-MB-231 cells transduced with the empty lentiviral vector; YWHAB, tyrosine 3-monooxygenase/tryptophan 5-monooxy-genase activation protein β; YWHAB-OE, MDA-MB-231 cells overexpressing *YWHAB*.

However, the pathways affected by *YWHAB* still require further research. Furthermore, it has been reported that a number of DEGs are associated with EMT. For example, *MMP1* improves the metastasis of MDA-MB-231 cells by promoting the EMT process (27). *MMP1* knockdown suppresses colorectal cancer progression by inhibiting EMT (28). *IL24* promotes bronchial EMT transformation in chronic asthma (29). *MMP3* is similar to *MMP1* in terms of affecting the EMT process, and *MMP3* promotes EMT in mouse mammary epithelial cells (30). The hemopexin domain of *MMP3* is responsible for mammary epithelial invasion, and the downregulation of *MMP3* inhibits breast tumor development (31,32). This indicates that downregulation of *MMP1* and *MMP3* inhibits EMT progression in breast cancer. In the present study, the expression levels of *MMP1*, *MMP3* and *IL24* were all downregulated after overexpression of YWHAB. Therefore, the effect of *YWHAB* on EMT was evaluated. The protein expression levels of the mesenchymal marker vimentin, epithelial marker E-cadherin and EMT transcription factor Slug were examined following overexpression of *YWHAB*. It was demonstrated that the expression of vimentin was decreased with the overexpression of *YWHAB* and increased after *YWHAB* knockdown. However, no significant changes were observed in the expression levels of E-cadherin and Slug (data not shown).

Vimentin is the major intermediate filament protein of mesenchymal cells and is ubiquitously expressed in normal mesenchymal cells (49). Reduction in mesenchymal characteristics can increase cell adhesion and ultimately reduce cell motility (50). Furthermore, another study reported that reduced vimentin levels can inhibit breast cancer cell metastasis (51). Consequently, the upregulation of *YWHAB* in breast cells could potentially result in the loss of mesenchymal cell characteristics and inhibit cell motility. There may be an association between *YWHAB* and vimentin, which requires further study.

In conclusion, the present study highlighted the inhibitory effect of *YWHAB* on breast cancer cell migration and invasion. We hypothesized that *YWHAB*, a regulatory gene associated with breast cancer, may reduce the mesenchymal characteristics of breast cancer cells and could serve as a promising
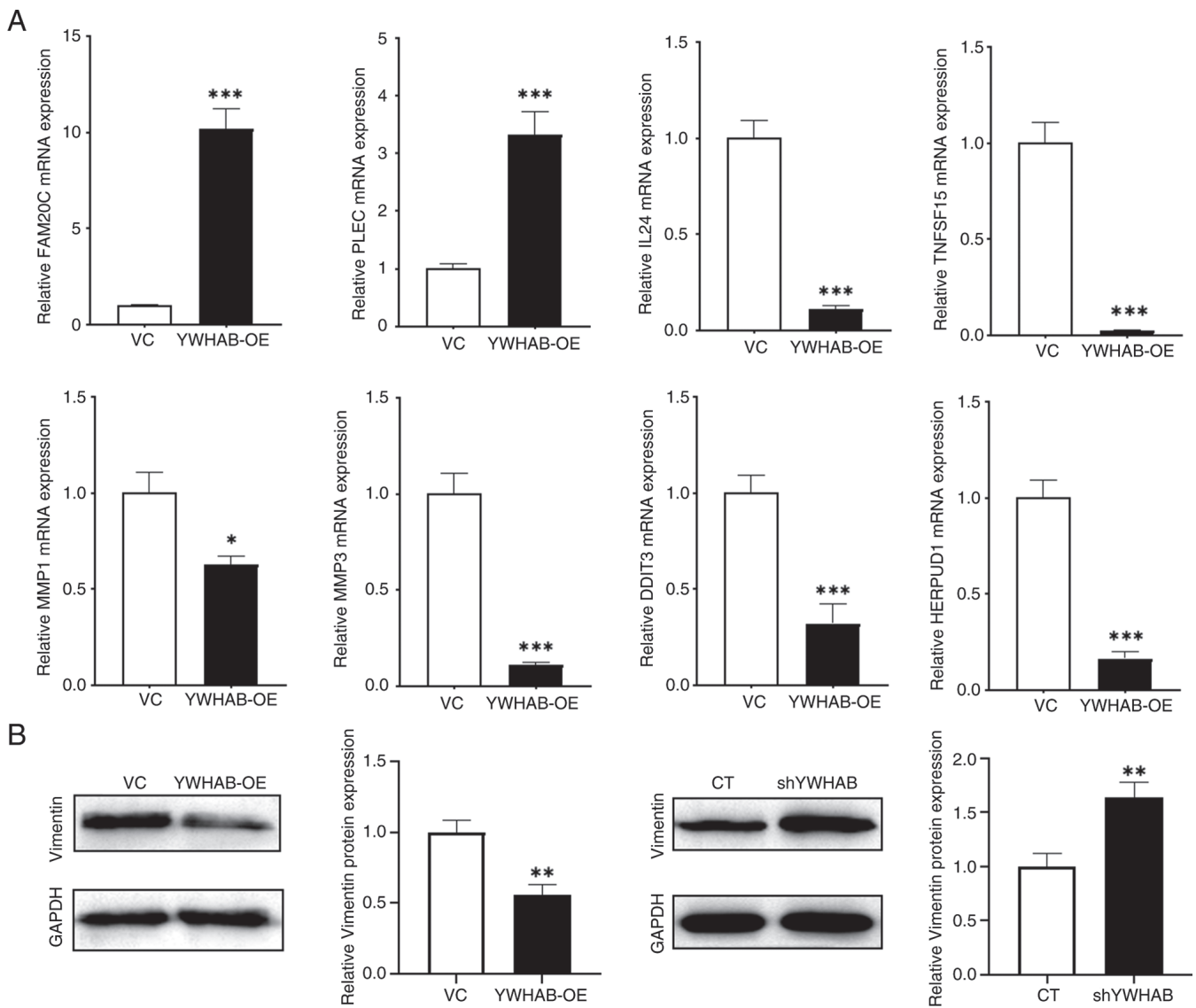
Figure 6. Expression levels of eight DEGs and epithelial-mesenchymal transition markers in breast cancer cell lines. (A) A total of eight DEGs from transcriptome sequencing were selected and verified using fluorescence reverse transcription-quantitative PCR in MDA-MB-231 cells. (B) Western blotting was used to detect the expression changes of vimentin when *YWHAB* was overexpressed in MDA-MB-231 cells and knocked down in MCF7 cells. *P<0.05, **P<0.01 and ***P<0.001. DEG, differentially expressed gene; YWHAB-OE, MDA-MB-231 cells overexpressing *YWHAB*; VC, MDA-MB-231 cells transduced with the empty lentiviral vector; shYWHAB, MCF7 cells with *YWHAB* knockdown; CT, MCF7 cells transduced with the lentiviral vector of scrambled negative control; YWHAB, tyrosine 3-monooxygenase/tryptophan 5-monooxygenase activation protein β.

therapeutic target. Furthermore, the results of the present study suggest that IRX5 may regulate *YWHAB* gene expression by affecting the *YWHAB* promoter. However, as the experiments performed in the present study were all performed *in vitro*, the effect of *YWHAB* on breast cancer metastasis *in vivo* also requires verification. Finally, the specific regulatory roles of IRX5 and *YWHAB* in breast cancer also require further study.

Availability of data and materials

The transcriptome data generated in the present study may be found in the Gene Expression Omnibus database under accession number GSE218458 or at the following URL: https://www.ncbi.nlm.nih.gov/geo/query/acc.cgi?acc=GSE218458. The other data generated in the present study may be requested from the corresponding author.

Authors' contributions

JL designed the study and supervised the data collection. JL and XG confirm the authenticity of all the raw data. XG, WX

and YS performed the experiments. JY and DZ performed the data analysis. XG and DZ wrote the manuscript, and JY, YS and XG revised the manuscript. All authors read and approved the final version of the manuscript.

Ethics approval and consent to participate

Not applicable.

Patient consent for publication

Not applicable.

Competing interests

The authors declare that they have no competing interests.

References

1. Siegel RL, Miller KD, Fuchs HE and Jemal A: Cancer statistics, 2022. CA Cancer J Clin 72: 7-33, 2022.
2. Sung H, Ferlay J, Siegel RL, Laversanne M, Soerjomataram I, Jemal A and Bray F: Global cancer statistics 2020: GLOBOCAN estimates of incidence and mortality worldwide for 36 cancers in 185 countries. CA Cancer J Clin 71: 209-249, 2021.
3. Wang L, Zhang S and Wang X: The metabolic mechanisms of breast cancer metastasis. Front Oncol 10: 602416, 2020.
4. Gui P: Evolution of metastasis: New tools and insights. Trends Cancer 8: 98-109, 2022.
5. Mehlen P and Puisieux A: Metastasis: A question of life or death. Nat Rev Cancer 6: 449-458, 2006.
6. Zeisberg M and Neilson EG: Biomarkers for epithelial-mesenchymal transitions. J Clin Invest 119: 1429-1437, 2009.
7. Zhang H, Meng F, Liu G, Zhang B, Zhu J, Wu F, Ethier SP, Miller F and Wu G: Forkhead transcription factor foxq1 promotes epithelial-mesenchymal transition and breast cancer metastasis. Cancer Res 71: 1292-1301, 2011.
8. Yan M, Wang J, Ren Y, Li L, He W, Zhang Y, Liu T and Li Z: Over-expression of FSIP1 promotes breast cancer progression and confers resistance to docetaxel via MRP1 stabilization. Cell Death Dis 10: 204, 2019.
9. Zhang J, Deng H and Wang J: LTBP1 promotes the progression of triple negative breast cancer via activating the RhoA/ROCK signaling pathway. Cancer Insight 3: 1-3, 2023.
10. Blazeck J and Alper HS: Promoter engineering: Recent advances in controlling transcription at the most fundamental level. Biotechnol 8: 46-58, 2013.
11. Petosa C, Masters SC, Bankston LA, Pohl J, Wang B, Fu H and Liddington RC: 14-3-3zeta binds a phosphorylated Raf peptide and an unphosphorylated peptide via its conserved amphipathic groove. J Biol Chem 273: 16305-16310, 1998.
12. Aghazadeh Y and Papadopoulos V: The role of the 14-3-3 protein family in health, disease, and drug development. Drug Discov Today 21: 278-287, 2016.
13. Gardino AK and Yaffe MB: 14-3-3 proteins as signaling integration points for cell cycle control and apoptosis. Semin Cell Dev Biol 22: 688-695, 2011.
14. Sime W, Niu Q, Abassi Y, Masoumi KC, Zarrizi R, Køhler JB and Massoumi R: BAP1 induces cell death via interaction with 14-3-3 in neuroblastoma. Cell Death Dis 9: 458, 2018.
15. Ou TT, Wang CJ, Lee YS, Wu CH and Lee HJ: Gallic acid induces G2/M phase cell cycle arrest via regulating 14-3-3β release from Cdc25C and Chk2 activation in human bladder transitional carcinoma cells. Mol Nutr Food Res 54: 1781-1790, 2010.
16. Komiya Y, Akiyama H, Sakumoto R and Tashiro F: FBI1/Akirin2 promotes tumorigenicity and metastasis of Lewis lung carcinoma cells. Biochem Biophys Res Commun 444: 382-386, 2014.
17. Cao L, Lei H, Chang MZ, Liu ZQ and Bie XH: Down-regulation of 14-3-3β exerts anti-cancer effects through inducing ER stress in human glioma U87 cells: Involvement of CHOP-Wnt pathway. Biochem Biophys Res Commun 462: 389-395, 2015.
18. Gong F, Wang G, Ye J, Li T, Bai H and Wang WW: 14-3-3beta regulates the proliferation of glioma cells through the GSK3beta/beta-catenin signaling pathway. Oncol Rep 30: 2976-2982, 2013.
19. Hu X, Bao M, Huang J, Zhou L and Zheng S: Identification and validation of novel biomarkers for diagnosis and prognosis of hepatocellular carcinoma. Front Oncol 10: 541479, 2020.
20. Livak KJ and Schmittgen TD: Analysis of relative gene expression data using real-time quantitative PCR and the 2(-Delta Delta C(T)) method. Methods 25: 402-408, 2001.
21. Smith T, Heger A and Sudbery L: UMI-tools: Modeling sequencing errors in Unique Molecular Identifiers to improve quantification accuracy. Genome Res 27: 491-499, 2017.
22. Kim D, Langmead B and Salzberg SL: HISAT: A fast spliced aligner with low memory requirements. Nat Methods 12: 357-360, 2015.
23. Pertea M, Pertea GM, Antonescu CM, Chang TC, Mendell JT and Salzberg SL: StringTie enables improved reconstruction of a transcriptome from RNA-seq reads. Nat Biotechnol 33: 290-295, 2015.
24. Liao Y, Smyth GK and Shi W: featureCounts: An efficient general purpose program for assigning sequence reads to genomic features. Bioinformatics 30: 923-930, 2014.
25. Love MI, Huber W and Anders S: Moderated estimation of fold change and dispersion for RNA-seq data with DESeq2. Genome Biol 15: 550, 2014.
26. Yu G, Wang LG, Han Y and He QY: clusterProfiler: An R package for comparing biological themes among gene clusters. OMICS 16: 284-287, 2012.
27. Zhu YH, Tao ZH, Chen Y, Lin SC, Zhu MG, Ji W, Liu XJ, Li T and Hu X: Exosomal MMP-1 transfers metastasis potential in triple-negative breast cancer through PAR1-mediated EMT. Breast Cancer Res Treat 193: 65-81, 2022.
28. Wang K, Zheng J, Yu J, Wu Y, Guo J, Xu Z and Sun X: Knockdown of MMP1 inhibits the progression of colorectal cancer by suppressing the PI3K/Akt/cmyc signaling pathway and EMT. Oncol Rep 43: 1103-1112, 2020.
29. Feng KN, Meng P, Zou XL, Zhang M, Li H, Yang HL, Li HT and Zhang TT: IL-37 protects against airway remodeling by reversing bronchial epithelial-mesenchymal transition via IL-24 signaling pathway in chronic asthma. Resp Res 23: 244, 2022.
30. Nelson CM, Khauv D, Bissell MJ and Radisky DC: Change in cell shape is required for matrix metalloproteinase-induced epithelial-mesenchymal transition of mammary epithelial cells. J Cell Biochem 105: 25-33, 2008.
31. Chu C, Liu X, Bai X, Zhao T, Wang M, Xu RC, Li MQ, Hu YY, Li WH, Liu H, et al: MiR-519d suppresses breast cancer tumorigenesis and metastasis via targeting MMP3. Int J Biol Sci 14: 228-236, 2018.
32. Correia AL, Mori H, Chen EI, Schmitt FC and Bissell MJ: The hemopexin domain of MMP3 is responsible for mammary epithelial invasion and morphogenesis through extracellular interaction with HSP90beta. Genes Dev 27: 805-817, 2013.
33. Iwatsuki M, Mimori K, Yokobori T, Ishi H, Beppu T, Nakamori S, Baba H and Mori M: Epithelial-mesenchymal transition in cancer development and its clinical significance. Cancer Sci 101: 293-299, 2010.
34. Gómez-Skarmeta JL and Modolell J: Iroquois genes: Genomic organization and function in vertebrate neural development. Curr Opin Genet Dev 12: 403-408, 2002.
35. Kim KH, Rosen A, Bruneau BG, Hui CC and Backx PH: Iroquois homeodomain transcription factors in heart development and function. Circ Res 110: 1513-1524, 2012.
36. Leyns L, Gómez-Skarmeta JL and Dambly-Chaudière C: iroquois: A prepattern gene that controls the formation of bristles on the thorax of Drosophila. Mech Develop 59: 63-72, 1996.
37. Marcinkiewicz KM and Gudas LJ: Altered epigenetic regulation of homeobox genes in human oral squamous cell carcinoma cells. Exp Cell Res 320: 128-143, 2014.
38. Huang L, Song F, Sun H, Zhang L and Huang C: IRX5 promotes NF-κB signalling to increase proliferation, migration and invasion via OPN in tongue squamous cell carcinoma. J Cell Mol Med 22: 3899-3910, 2018.
39. Myrthue A, Rademacher BL, Pittsenbarger J, Kutyba-Brooks B, Gantner M, Qian, DZ and Beer TM: The iroquois homeobox gene 5 is regulated by 1,25-dihydroxyvitamin D3 in human prostate cancer and regulates apoptosis and the cell cycle in LNCaP prostate cancer cells. Clin Cancer Res 14: 3562-3570, 2008.
40. Zhu L, Dai L, Yang N, Liu M, Ma S, Li CC, Shen J, Lin T, Wang D, Pan W and Li X: Transcription factor IRX5 promotes hepatocellular carcinoma proliferation and inhibits apoptosis by regulating the p53 signalling pathway. Cell Biochem Funct 38: 621-629, 2020.

41. Zhu Q, Wu Y, Yang M, Wang Z, Zhang H, Jiang XL, Chen M, Jin TY and Wang T: IRX5 promotes colorectal cancer metastasis by negatively regulating the core components of the RHOA pathway. Mol Carcinog 58: 2065-2076, 2019.
42. Hua Y, Wang H, Wang H, Wu X, Yang L, Wang CL, Li X, Jin YH, Li M, Wang L, *et al*: Circular RNA Circ_0006282 promotes cell proliferation and metastasis in gastric cancer by regulating MicroRNA-144-5p/Tyrosine 3-Monooxygenase/Tryptophan 5-Monooxygenase activation protein β axis. Cancer Manag Res 13: 815-827, 2021.
43. Li C, Li Z and Zhang M: Low Expression of 14-3-3beta is associated with adverse survival of diffuse large B-Cell lymphoma patients. Front Med (Lausanne) 6: 237, 2019
44. Wu YJ, Jan YJ, Ko BS, Liang SM and Liou JY: Involvement of 14-3-3 proteins in regulating tumor progression of hepatocellular carcinoma. Cancers 7: 1022-1036, 2015.
45. Liu TA, Jan YJ, Ko BS, Chen SC, Liang SM, Hung YL, Chiun H, Shen TL, Lee YM, Chen PF, *et al*: Increased expression of 14-3-3β promotes tumor progression and predicts extrahepatic metastasis and worse survival in hepatocellular carcinoma. Am J Pathol 179: 2698-2708, 2011.
46. Tang Y, Lv P, Sun Z, Han L and Zhou W: 14-3-3β promotes migration and invasion of human hepatocellular carcinoma cells by modulating expression of MMP2 and MMP9 through PI3K/Akt/NF-κB pathway. PLoS One 11: e0146070, 2016.
47. Zhang X, Zhang Q, Zhang K, Wang F, Qiao X and Cui JQ: Circ SMARCA5 inhibited tumor metastasis by interacting with SND1 and downregulating the *YWHAB* gene in cervical cancer. Cell Transplant 30: 963689720983786, 2021.
48. Hanahan D and Weinberg RA: Hallmarks of cancer: The next generation. Cell 144: 646-674, 2011.
49. Driskell RR, Lichtenberger BM, Hoste E, Kretzschmar K, Simons BD, Charalambous M, Ferron SR, Herault Y, Pavlovic G, Ferguson-Smith AC and Watt FM: Distinct fibroblast lineages determine dermal architecture in skin development and repair. Nature 504: 277-281, 2013.
50. Lohneis P, Sinn M, Klein F, Bischoff S, Striefler JK, Wislocka L, Sinn BV, Pelzer U, Oettle H, Riess H, *et al*: Tumour buds determine prognosis in resected pancreatic ductal adenocarcinoma. Br J Cancer 118: 1485-1491, 2018.
51. Calaf GM, Balajee AS, Montalvo-Villagra MT, Leon M, Navarrete M D, Alvarez RG, Roy D, Narayan G and Jorge AQ: Vimentin and Notch as biomarkers for breast cancer progression. Oncol Lett 7: 721-727, 2014.